Cytoplasmic Motions, Rheology, and Structure Probed by a Novel Magnetic Particle Method

PETER A. VALBERG* and DAVID F. ALBERTINI‡
*Department of Environmental Science and Physiology, Harvard School of Public Health, Boston, Massachusetts 02115; and ‡Department of Anatomy and Cellular Biology, Tufts University School of Medicine, Boston, Massachusetts 02111.

ABSTRACT The motions of magnetic particles contained within organelles of living cells were followed by measuring magnetic fields generated by the particles. The alignment of particles was sensed magnetometrically and was manipulated by external fields, allowing non-invasive detection of particle motion as well as examination of cytoplasmic viscoelasticity. Motility and rheology data are presented for pulmonary macrophages isolated from lungs of hamsters 1 d after the animals had breathed airborne γ-Fe_2O_3 particles. The magnetic directions of particles within phagosomes and secondary lysosomes were aligned, and the weak magnetic field produced by the particles was recorded. For dead cells, this remanent field was constant, but for viable macrophages, the remanent field decreased rapidly so that only 42% of its initial magnitude remained 5 min after alignment. A twisting field was applied perpendicular to the direction of alignment and the rate at which particles reoriented to this new direction was followed. The same twisting was repeated for particles suspended in a series of viscosity standards. Based on this approach, the low-shear apparent intracellular viscosity was estimated to be 1.2–2.7 $\times$ 10^3 Pa·s (1.2–2.7 $\times$ 10^4 poise). Time-lapse video microscopy confirmed the alignment of ingested particles upon magnetization and showed persistent cellular motility during randomization of alignment. Cytochalasin D and low temperature both reduced cytoplasmic activity and remanent-field decay, but affected rheology differently. Magnetic particles were observed in association with the microtubule organizing center by immunofluorescence microscopy; magnetization did not affect microtubule distribution. However, both vimentin intermediate filaments and f-actin reorganized after magnetization. These data demonstrate that magnetometry of isolated phagocytic cells can probe organelle movements, rheology, and physical properties of the cytoskeleton in living cells.

Definition of the structure and physical properties of cytoplasm within living cells is essential to a more complete understanding of cellular function. As recently reviewed by Porter (27), structure of the cytoplasmic matrix has been the subject of intense study and debate for many years, and current advances in cellular biology have contributed substantially towards an integrated model of how the formed elements of cytoplasm regulate diverse cellular processes. The cytomatrix has emerged as a likely site for regulation of cytoplasmic viscosity (22, 29), cellular and intracellular motions (16, 25, 30, 36), and cellular shape (1, 12, 18). However, techniques have not been available to relate these functions to physical properties of the cytomatrix in living cells. One approach for directly quantifying cytoplasmic motility and rheology is to magnetometrically detect the movements of magnetic particles that have been phagocytized by cells. The motion of such particles within cells was studied optically by Crick and Hughes (10) and was first detected magnetometrically in human subjects by Cohen (6). The magnetometric approach for assessing particle motion has recently been applied both to intact animals (4, 15) and to isolated cells (37).

Magnetic particles can be used to monitor spontaneous cytoplasmic activity without the need for optical observation. Furthermore, external fields can be used to apply a torque to aligned particles, and the rate of particle rotation is a measure of apparent intracellular viscosity (or resistance to rotation),

THE JOURNAL OF CELL BIOLOGY · VOLUME 101 JULY 1985 130-140

in the local environment of the particle. We describe the results of magnetometric measurements made on isolated lung macrophages for the purpose of detecting intracellular motions and estimating local apparent viscosity. To analyze the possible structural basis for magnetometrically sensed motion, we evaluated the effects of magnetization on the organization of the cytoskeleton. The combined magnetometric and morphological studies suggest that specific cytoplasmic components may be responsible for the type of motions probed with this system.

MATERIALS AND METHODS

Pulmonary macrophages were tagged with γ-Fe_2O_3 (maghemite) particles by having hamsters (n=16) breathe airborne particulates generated by a previously described technique (38). Briefly, iron pentacarbonyl vapors were oxidized under controlled conditions to produce an aerosol of maghemite particles at a concentration of ~300 μg/liter (aerodynamic mean diameter = 0.7-μm, aggregates of γ-Fe_2O_3 with 0.1-μm diameter subunits). Some of the inhaled material deposits on lung surfaces and almost all of the particles retained in alveoli are ingested by macrophages within 12–24 h (31–33). 1 d after inhalation exposure, pulmonary macrophages were harvested by multiple saline washes of the lungs. Each hamster was anesthetized with an intraperitoneal injection of pentobarbital sodium (50 mg/kg body wt), after which the trachea was exposed and cannulated with PE-190 tubing attached to an 18-gauge syringe needle. The lungs were lavaged 13 times with 3-ml aliquots of normal saline. The lack of divalent cations promotes detachment of macrophages from the alveolar surface, and gentle massage of the chest further increases cell yield (39). The first wash was discarded because of a high content of mucus, surfactant, and cell debris; the remaining washes were pooled and the macrophages were pelleted by centrifugation (100 g, 10 min). Cells were counted and sized by Coulter counter (Coulter Electronics Inc., Hialeah, FL), and the yield of cells lavaged from Syrian hamster lungs was 4–8 × 10^6 macrophages per animal with a viability of 85–94% as determined by dye exclusion. The particle content of macrophages was ~20 μg γ-Fe_2O_3 per 10^6 cells, as measured by magnetometry.

Cells were resuspended in Roswell Park Memorial Institute 1640 medium with 0.2% bovine serum albumin (BSA) and 25 mM HEPES buffer at 37°C. The macrophages were divided into separate portions, and each aliquot of 10^6 cells was allowed to adhere to the bottom of 1.5-ml glass vials over a period of 1 h. The cells in each vial were incubated for an additional 1/2 h under one of the five following conditions: (*a*) 37°C, control; (*b*) 37°C and 20 μM cytochalasin D, 0.2% dimethyl sulfoxide; (*c*) 37°C and 0.2% dimethyl sulfoxide; (*d*) 10°C; (*e*) 37°C and 10% Formalin. Motion of the intracellular particles was then magnetometrically measured for the attached macrophages in each vial.

Ferromagnetic particles become magnetized when a strong external magnetic field is applied, and they produce a new field after the external field has been removed. This new field is called the remanent field and is maintained indefinitely in magnitude and direction unless the individual particles rotate. Thus, when a magnetic field is applied briefly to intracellular particles, the magnetic directions of these particles are aligned, and they produce a remanent field, proportional to the total mass of particles. The remanent magnetic field decreases only if the particle orientation becomes randomized away from the initial direction of alignment. During observation of cells with a microscope, a permanent magnet was used as a magnetic field source so as to produce a visual signal, i.e., alignment of the long axis of the magnetic particles along the field lines of the magnet.

For the magnetometric measurements of motility and apparent viscosity, alignment of the ingested particle magnetic moments was produced by a brief pulse (10 μs) of a homogeneous 0.1 T (tesla) [=1,000 G (gauss)] magnetizing field. This was preferable to using a permanent magnet, as done in previous magnetometric studies (4, 14, 15, 37), because, as we have shown here, application of the permanent magnet physically rotates the particles and enhances magnetic particle aggregation. The short duration of the 10-μs pulse does not permit particle movement even in a fluid with viscosity as low as water.

The weak remanent field produced by the cell-associated particles was detected using the apparatus shown in Fig. 1, which incorporated the noise-reduction and signal enhancement capabilities necessary to detect weak remanent fields (~4 nT = 40 μG) in the presence of much larger environmental magnetic fields (~10^4 nT = 0.1 G). The remanent magnetic field was sensed with a Förster 1.107 fluxgate magnetometer (Förster Instruments, Inc., Corapolis, PA) with two pairs of low-noise field and gradient probes connected in a second-order gradiometer configuration (see Fig. 1). All four probes were oriented parallel to field lines from the cells and internalized particles to optimize their sensitivity to this magnetic field; but perturbing fields from distant sources produced signals of opposite polarity in each probe pair, yielding minimal output. The pulse magnetization was along the direction indicated by the arrows on the outer probes; this aligned the magnetic domains of the particles, and the probes could sense the remanent field. The cells and the vial containing them were turned about a vertical axis at ~10–13 rotations per second. This rotation was part of the signal-enhancement scheme and produced only a small centrifugal force on the cells (~1/2 g). A phase-sensitive amplifier combined the magnetometer signal with a reference signal synchronized to cell vial rotation and amplified only those signals in synchrony with sample rotation. The implementation of these techniques made the apparatus optimally sensitive to the local magnetic field from the cells and served to cancel magnetic noise from outside sources.

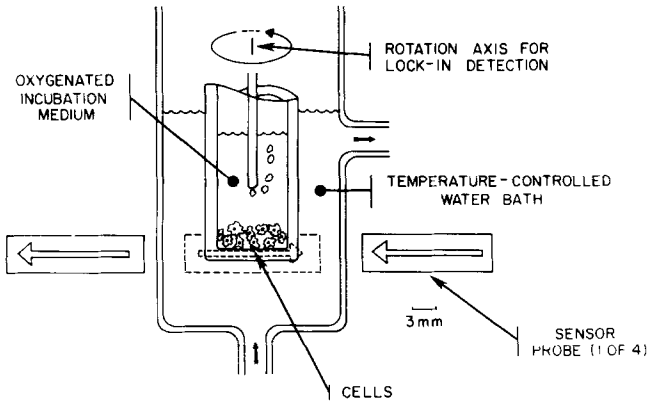

FIGURE 1 Illustration of the apparatus design for measuring remanent field decay in living macrophages that contain maghemite particles. Cells were adherent to the bottom and sides of glass vials containing incubation medium that was oxygenated by a flow of air plus 5% CO_2. The temperature of the cells and incubation medium was maintained by a circulating water bath. The cells and the vial containing them were rotated about a vertical axis at ~13 Hz. Magnetic signals were sensed by four fluxgate magnetometer probes, and amplification was locked to the 13-Hz rotation rate to detect only the cell signal and to reject noise at other frequencies arising from environmental magnetic fields.

Intracellular apparent viscosity was probed by first magnetically aligning the ingested particles with a brief pulse, and subsequently applying a magnetic field along the axis of cell vial rotation, i.e., perpendicular to the direction in which the particles had been aligned by magnetization. The magnitude of this right-angle field (2.5 mT = 25 G) was much smaller than the pulsed magnetizing field and did not alter the intrinsic magnetization of the particles. However, the magnetic particles behave as compass needles and slowly reorient toward the "twisting" field, and the amount of remanent field the fluxgate probes sense decreases. The remanent field signal can be related to the time course of particle rotation, and the rate at which particles rotate is determined by both the strength of the twisting field and the apparent viscosity of the medium which retards particle rotation. To calibrate these measurements, we suspended, in viscosity standards, samples of the same particles that were used to load the cells (Dow Corning dimethylpolysiloxane 200 fluid, Dow Corning Corp., Midland, MI) ranging from 60 Pa·s to 600 Pa·s (1 Pa·s = 10 poise) and these particles were twisted in the same manner as intracellular particles. This procedure served to correct for the fact that particle clumps contained nonmagnetic volume which contributed to hydrodynamic size but not to remanent magnetization. Particles were also mixed with and embedded in Epon and were thin-sectioned and examined in a transmission electron microscope.

Particle rotation as a method of probing intracellular apparent viscosity has advantages over experiments that pull magnetic spheres within cells (17, 28, 29, 43): considerably smaller particle clusters (of the same size as organelles) can be used, and the particles are twisted while in one area of the cell. No translocation across cytoplasmic structures is required. Hydrodynamic corrections for effects of particle size and shape and for effects of cell boundaries are less severe than when using particle translocation (20).

For video microscopy, macrophages adherent to glass coverslips (37°C, 1 h) were inverted on a drop of culture medium and sealed on a glass slide with Vaseline. Cells and their internalized particles were placed on the stage of a Zeiss Photoscope III maintained at 37°C and were viewed under bright field, phase-contrast, or Nomarski differential-interference contrast optics. Nomarski

optics were used for observations of cell movement, whereas bright field conditions were optimal for viewing the disposition of the rust-brown iron oxide particles. For magnetization, a permanent magnet (0.2 T = 2,000 G) was placed at the edge of the slide so as to have field lines parallel to the specimen plane; the magnet was left on the stage for 2–3 min to produce magnetic and physical alignment of intracellular particles. The disposition of particles was analyzed before, during, and after magnetization by time-lapse video microscopy using a DV-2 Venus Scientifics camera; real-time recordings were made on a Panasonic time-lapse recorder (NV-8030), and cell and particle behavior was visualized on a Conrac (SN/9) monitor.

To evaluate cytoskeletal organization, coverslip-adherent cells (37°C, 1 h) were fixed before and after magnetization with a permanent magnet and stained with previously characterized anti-tubulin (13), or anti-vimentin (18) antisera or rhodamine-conjugated phalloidin for f-actin (2). For anti-tubulin staining, cells were plunged into −20°C methanol for 10 min, washed in PBS, labeled with rabbit anti-tubulin serum (1:100 dilution in PBS) for 60 min at 37°C, washed in PBS, and stained with rhodamine goat anti-rabbit immunoglobulin (lot. # S164) (Miles Ames Div., Miles Laboratories Inc., Elkhart, IN) for 1 h at 37°C. Phalloidin and anti-vimentin staining was done on cells fixed for 10 min at 25°C in a 3.7% formaldehyde solution of 0.1 M PIPES (pH 6.9), 0.1% Nonidet P-40, 0.1% Aprotinin (Sigma Chemical Co., St. Louis, MO), 1.0 mM EGTA, 2.5 mM $MgCl_2$, and 50% deuterium oxide. F-actin was stained by incubating the cells for 15 min at 37°C in 1 unit (per 100 μl of PBS) of rhodamine-phalloidin (Molecular Probes Inc., Junction City, OR). To label intermediate filaments, we incubated cells with anti-vimentin antiserum (diluted 1:100 in PBS) for 1 h at 37°C, washed them in PBS, and labeled them with rhodamine goat anti-rabbit IgG as above. Coverslips were mounted on glass slides in a drop of 50% glycerol containing Hoechst 33258 (Polysciences, Inc., Warrington, PA) to counterstain nuclei. The epiillumination system of a Zeiss Photoscope III was used in combination with the rhodamine filter set to observe labeled cytoskeletal elements. The intracellular iron oxide itself did not produce any fluorescence signal at the rhodamine wavelength. Photographs were recorded on 35-mm Kodak Tri-X film push processed to 1200 ASA using acufine developer. Both cells with aligned particles and with unaligned particles were examined.

Lavaged cells were also prepared for examination by electron microscopy. Both nonmagnetized and magnetized cells were pelleted, fixed (2.5% glutaraldehyde in 0.16 M potassium phosphate buffer for 1 h at 24°C, postfixed with 1% OsO_4 in 0.1 M sodium cacodylate), dehydrated in graded series of ethanols, infiltrated with propylene oxide, and embedded in Epon. Thin sections from pellets of control and magnetized cells were stained with uranyl acetate and lead citrate and examined in a Philips 300 transmission electron microscope. Fifty-nine nucleated cell profiles of both magnetized and nonmagnetized cells were examined. For magnetized cells, it was important to be aware of the orientation of the cell pellet relative to the direction of magnetization during embedment and sectioning. Sections were cut in the same plane as the direction of magnetization, but perpendicular to line of magnetization in this plane. This assured that the particle chains seen were not an artifact of sectioning.

RESULTS

Particle Behavior in Living Cells

The magnetic iron oxide particles were resolved in living cells under bright field and Nomarski optics. As shown in Fig. 2, *A* and *B*, variable numbers of particles were found within single cells. In heavily loaded cells, the particles accumulated in a perinuclear region, whereas a more random particle disposition was seen in less loaded cells. Application of a permanent magnet caused particle alignment within cells (Fig. 2, *C* and *D*) without affecting cellular translocation and ruffling activity. After removal of the magnet, cytoplasmic movements continued, and within 3–5 min alignment of the particles was randomized (Fig. 2, *E* and *F*). Subsequent to magnetization, the particles tended to remain aggregated in chains, usually in a perinuclear position.

Time-lapse videotape recordings of cells maintained at 37°C showed alignment of the particles within 10–20 s after the magnet was applied, and, upon removal of the magnet, a gradual loss of alignment. The cells remained quite active during and after magnetization as evidenced by formation and retraction of pseudopods, persistent membrane ruffling, and a limited degree of translocation along the substrate. Occasionally, a polymorphonuclear leukocyte was seen among the lung macrophages. The neutrophils exhibited considerably faster locomotory movement than macrophages. Replay of video recordings showed that alignment with the permanent magnet caused maghemite-containing organelles within a single cell to link up in chains parallel to magnetic field lines. After removal of the magnet, these chains would bend and twist, but generally did not break up. Cells with only a few, small ingested particles showed continued translational movements of particle-containing organelles during and after magnetization. Particles in formalin-fixed cells could be magnetically oriented, but, in contrast to living cells, the alignment produced was stable and unchanging.

Electron micrographs (Fig. 3, *A–C*) showed that the electron-dense γ-Fe_2O_3 particles were confined to membrane-bound organelles having the appearance of phagosomes or secondary lysosomes. The micrographs show cells which had either not been magnetized (Fig. 3, *A* and *C*) or cells which had been fixed after particle alignment with a permanent magnet (Fig. 3, *B* and *C* [inset]). Although the alignment and aggregation of particles within organelles was strikingly apparent in thin sections, it was difficult to define membrane boundaries in magnetized samples (Fig. 3 *B*). Resin impregnation in such regions was often incomplete and the hard and abrasive particles resisted sectioning. Voids were created in the resin where particles fell out (Fig. 3, *A* and *B*). The linkage of individual particles into chains upon magnetization could distinctly be seen (Fig. 3, *B* and *C* [inset] arrows), and these aggregates were quite prominent in the perinuclear area. Frequently, particle-containing organelles were situated in proximity to the Golgi complex (Fig. 3 *C*), and bundles of 10-nm filaments were evident in this region. The size distribution of particle clusters in cells not magnetized with the permanent magnet was determined from electron micrographs, and the average cluster diameter was calculated to be 0.64 ± 0.30(SD)μm (41).

Cytoskeletal Organization

To evaluate effects of the particle twisting that accompanies application of the permanent magnet, we performed fluorescence microscopy on cells before and after magnetization. Organization of the cytoskeleton was visualized using indirect immunofluorescence staining for tubulin- and vimentin-containing structures and using phalloidin to stain filamentous actin. The indirect immunofluorescence staining pattern with anti-tubulin is characterized by the presence of many fibrillar structures, presumably microtubules, radiating from a single microtubule-organizing center adjacent to the nucleus (Fig. 4, *A* and *B*). As noted earlier, ingested particles accumulate in the cell center near the microtubule-organizing center. Upon particle alignment with the permanent magnet, no change in the pattern of anti-tubulin staining was apparent (Fig. 4, *C* and *D*) since cells on the same coverslip exhibited identical patterns regardless of the presence of aligned particles. In contrast, actin microfilaments, and to a lesser extent vimentin intermediate filaments, were both modified in distribution as a result of magnetization. Cells not treated with the permanent magnet and labeled with rhodamine phalloidin exhibited a generally diffuse cytoplasmic staining and well-delineated areas of stain which coincided with membrane ruffles (Fig. 5, *A* and *B*). Although phalloidin stain was

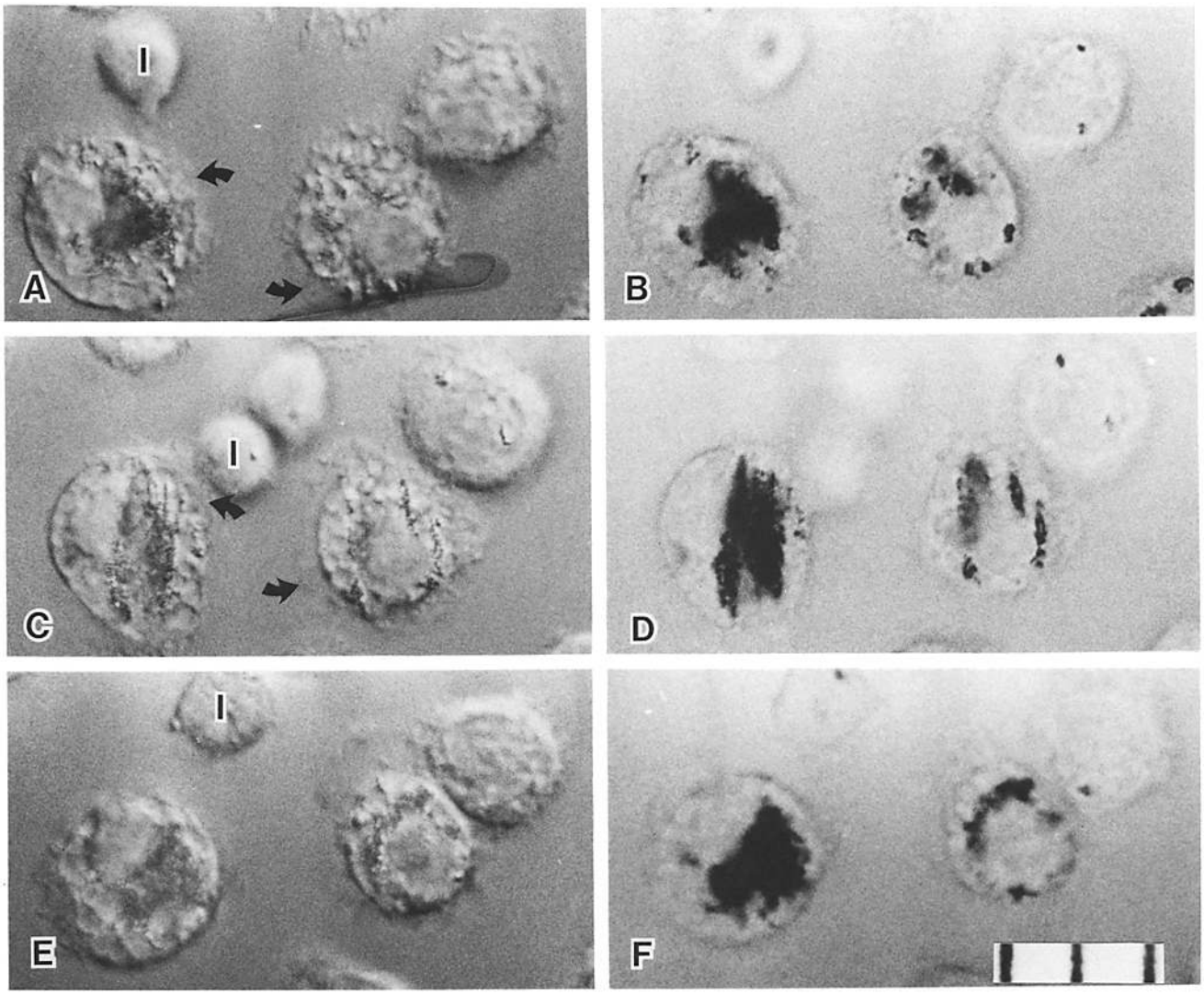

FIGURE 2 Corresponding micrographs of living hamster alveolar macrophages, taken under Nomarski (*left*) and bright field optics (*right*) before (*A* and *B*), during (*C* and *D*), and after (*E* and *F*) magnetization with an externally applied permanent magnet. Before magnetization, ingested particles exist as perinuclear aggregates or are dispersed throughout the cytoplasm (*A* and *B*); individual particles become aligned into vertical rows upon application of a permanent magnet with field lines running vertically in the plane of these micrographs (*C* and *D*). Note that membrane ruffling along the cell borders (arrows, *A* and *C*) continues, and that the position of the cells has not changed significantly. After the magnet is removed (*E* and *F*), ruffling activity continues and the particles remain aggregated around the nucleus. A leukocyte (*l*) is seen actively migrating near the macrophages. Bar, 10-μm divisions.

unevenly distributed or patchy in some untreated cells, there was little correspondence of the distribution of f-actin with the location of ingested particles. However, upon particle alignment, two changes in phalloidin staining were noted. The cell margin was regularly stained with areas of ruffling being the most intensely labeled (Fig. 5 *D*). The most conspicuous alteration was the appearance of prominent patches of phalloidin staining which spatially coincided with the location of aligned particles (compare Fig. 5, *C* and *D*). The appearance of phalloidin patches was confined to cells containing particles, suggesting that as a result of alignment, local changes in the organization of f-actin were induced.

Previous studies have shown that cultured mouse macrophages form perinuclear coils of intermediate filaments (24). Perinuclear aggregates of ingested particles were typically located within intermediate filament coils in hamster lung macrophages (Fig. 5, *E* and *F*). As a result of particle alignment with the permanent magnet, the appearance of the intermediate filaments was altered in the sense that the bundles noted in magnetized cells were not as clearly demarcated, as evidenced by a diffuse perinuclear stain (Fig. 5, *G* and *H*). Staining intensity was not diminished in samples prepared from three different experiments suggestive of some degree of rearrangement of the filaments comprising the perinuclear bundles. Higher resolution images of this region, using electron microscopy, will be needed to clarify the organization of intermediate filaments in relation to particle alignment. It should be noted, however, that transmission electron micrographs of the perinuclear region do demonstrate intermediate filament aggregates associated with ingested particles (Fig. 3 *C*).

Magnetometric Measurement of Motility and Viscosity

Figs. 6, *A–C*, are representative recordings of the remanent

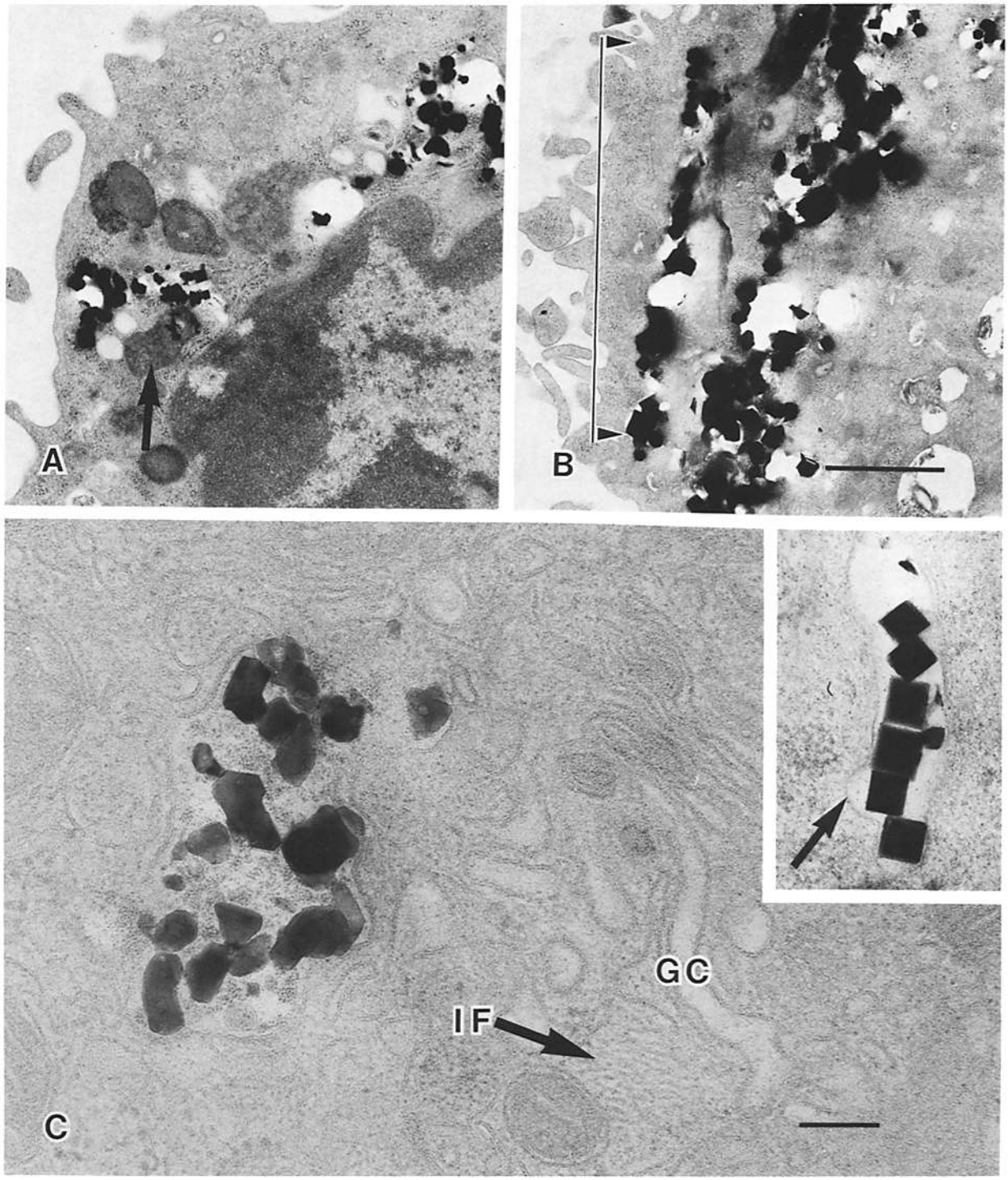

FIGURE 3 Transmission electron micrographs of hamster alveolar macrophages containing maghemite particles. *A* illustrates a portion of a control (nonmagnetized) cell in which particles occupy numerous perinuclear vacuoles, including a densely stained secondary lysosome (arrow). In *B*, a portion of a macrophage subjected to magnetization for 2 min with a permanent magnet, showing the alignment of particle-bearing phagosomes into chains (arrows). The magnetization field lines were in the plane of the section and running vertically. The voids in *A* and *B* correspond to areas where particles fell out of the section. At higher magnification, as shown in *C*, maghemite particles are shown collected within a single membrane-limited phagosome; this phagosome is situated near the Golgi complex (*GC*) and a bundle of intermediate filaments (*IF*). The inset in *C* illustrates the alignment of particles within an endocytic invagination of the cell surface which bears a coated pit (arrow). *A* and *B*, ×19,000; *C* and *inset*, ×61,500. Bar, 1 μm (*B*); and 200 nm (*C*).

magnetic field after pulse magnetization from particle-containing cells incubated in the magnetometry apparatus shown in Fig. 1. In each graph, the upper curve (R) shows the spontaneous decrease of the remanent field in living cells with no external force applied; the lower curve ($R + T$) was produced when a twisting field of 2.5 mT (or 25 G) was applied perpendicular to the original direction of magnetization. First, we present the effects of spontaneous cell move-

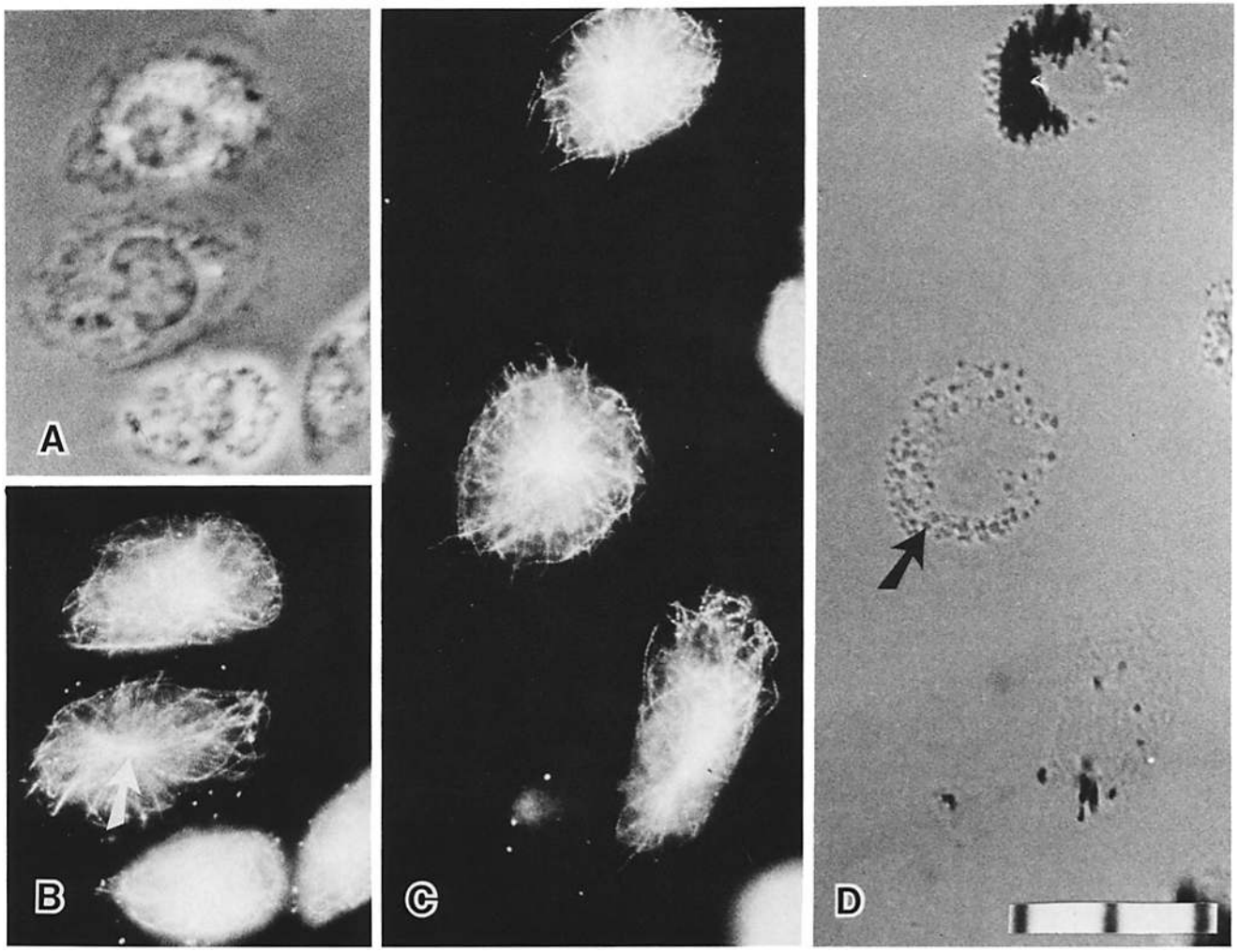

FIGURE 4 Macrophage anti-tubulin staining patterns before and after application of a permanent magnet. Before magnetization, phase-lucent particles are located adjacent to nuclei as shown in *A*; the corresponding anti-tubulin pattern (*B*) illustrates many microtubules emanating from a single microtubule-organizing center (arrow). This pattern remains unchanged after magnetization (*C*) when particles exhibit alignment (*D*); the cell indicated by the arrow in *D* does not contain ingested particles. Bar, 10-μm divisions.

ments on the time course of the remanent field.

If cells were formalin-fixed, the remanent field was constant (data not shown), but for oxygenated macrophages at 37°C, the field decreased rapidly (Fig. 6*A*, curve *R*) to 42% of its initial value in 5 min. Since the magnetization of each particle is permanent, the spontaneous decrease in remanent field seen for living cells is due to random rotation of individual particles away from their original direction of magnetization as driven by active cytoplasmic rearrangements that move and reorient the particle-containing organelles. The remanent field decay is slowed by either cooling the cells to 10°C (Fig. 6*B*, curve *R*), or by incubation in 20 μM cytochalasin D for 1/2 h prior to magnetization (Fig. 6*C*, curve *R*). Dimethyl sulfoxide alone had no effect (data not shown). Video recordings confirmed that these treatments inhibit active movements within the cytoplasm.

The externally applied twisting force causes reorientation to occur more rapidly as evidenced by the increased decay rate for the remanent field ($R + T$ curves). Moreover, a dramatic difference can be seen in the effect of a twisting force on each preparation; cooled cytoplasm resists shear, but cytochalasin D–treated cytoplasm does not (contrast the $R + T$ curves in Figs. 6, *B* and *C*). Elastic recoil was also observed, as illustrated in Fig. 6*D*. Here, the twisting field was applied for 1 min during the interval between the two arrows. The yield upon force application and corresponding recoil after force removal is evident in the recording. The $R + T$ curves for normal cells (e.g. Fig. 6*A*) were assumed to be the product of spontaneous reorientation and driven reorientation. The reorientation due to twist alone can then be generated by dividing the $R + T$ curve by the R curve. By comparing the resulting curve to the curves obtained when twisting particles suspended in a series of viscosity standards, it was calculated that the apparent cytoplasmic viscosity for these particles within oxygenated cells at 37°C ranges from 1.2 kPa·s (12,000 poise) at shear rates of 0.003 s^{-1} to 2.7 kPa·s (27,000 poise) at shear rates of 0.001 s^{-1} (viscosity of H_2O at 37°C = 0.0007 Pa·s = 0.007 poise). The cytoplasm is undoubtedly a non-Newtonian viscous fluid in that the observed viscosity will depend on the rate of shear, the size of the moving object, and the history of shear. However, the shear rates applied here were comparable to observed spontaneous particle motions in cells in that remanent field decay rates were approximately doubled, and the particle size was comparable to the size of intracellular organelles (~0.3–0.9 μm diameter).

The intracellular particle clusters exist in a distribution of

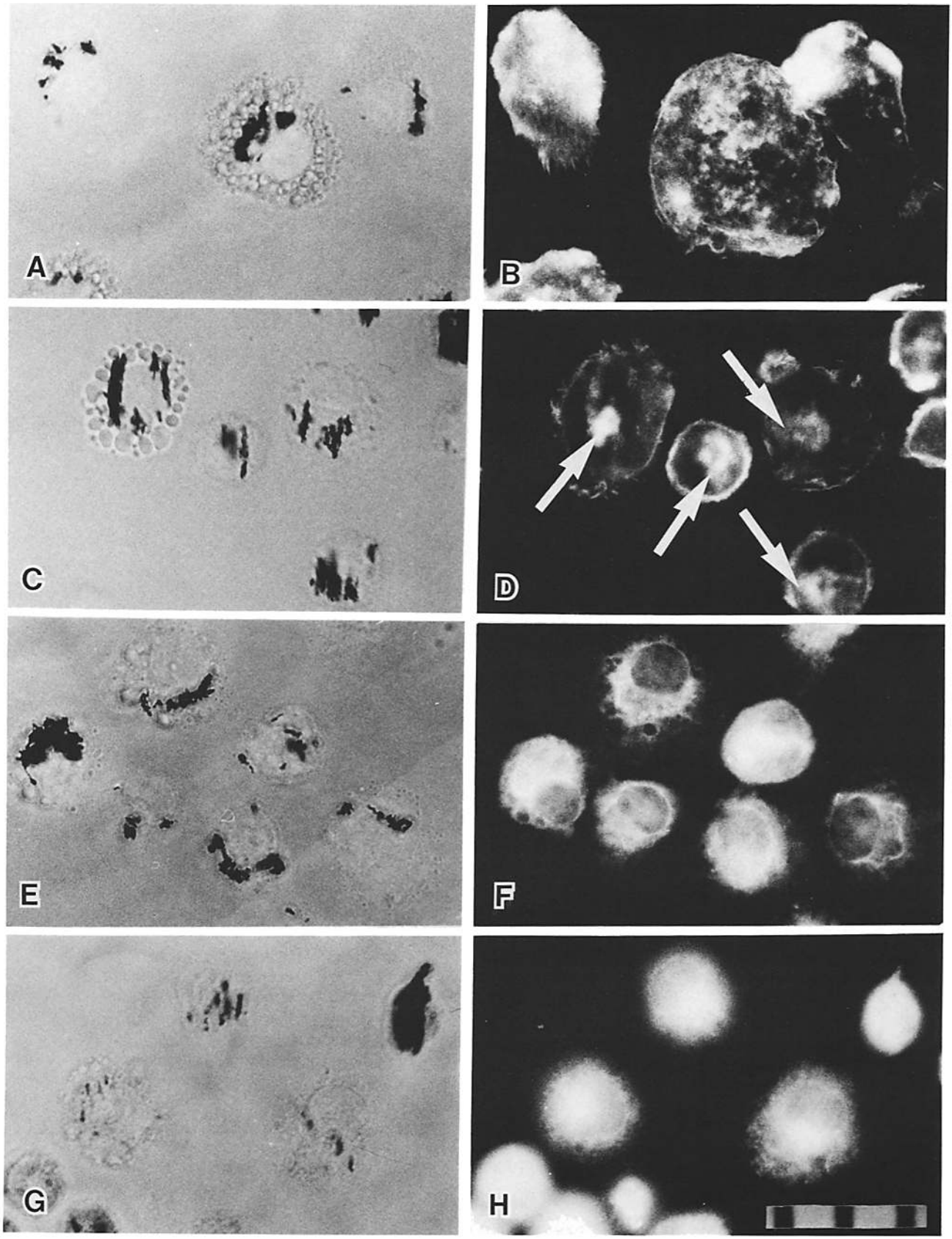

FIGURE 5 Shown are corresponding bright field (*left*) and fluorescence (*right*) micrographs of alveolar macrophages before (*A*, *B*, *E*, and *F*) and after (*C*, *D*, *G*, and *H*) permanent magnet magnetization. Control cells exhibit perinuclear particles (*A*) while rhodamine-phalloidin staining (*B*) shows that F-actin is concentrated in the cortex and diffusely localized throughout the cytoplasm. A different field of cells is shown in *C* and *D* where particles have become aligned and phalloidin staining is prominent in central patches, which correspond to areas occupied by magnetic particles (arrows, *D*; compare with *C*). In *E*, central particle aggregates coincide in distribution with bundles of intermediate filaments demonstrated by indirect immunofluorescence with anti-vimentin antibody (*F*). After magnetization (*G*), aligned particles remain associated with foci of anti-vimentin staining (*H*) although the filament bundles are not well defined. Bar, 10-μm divisions.

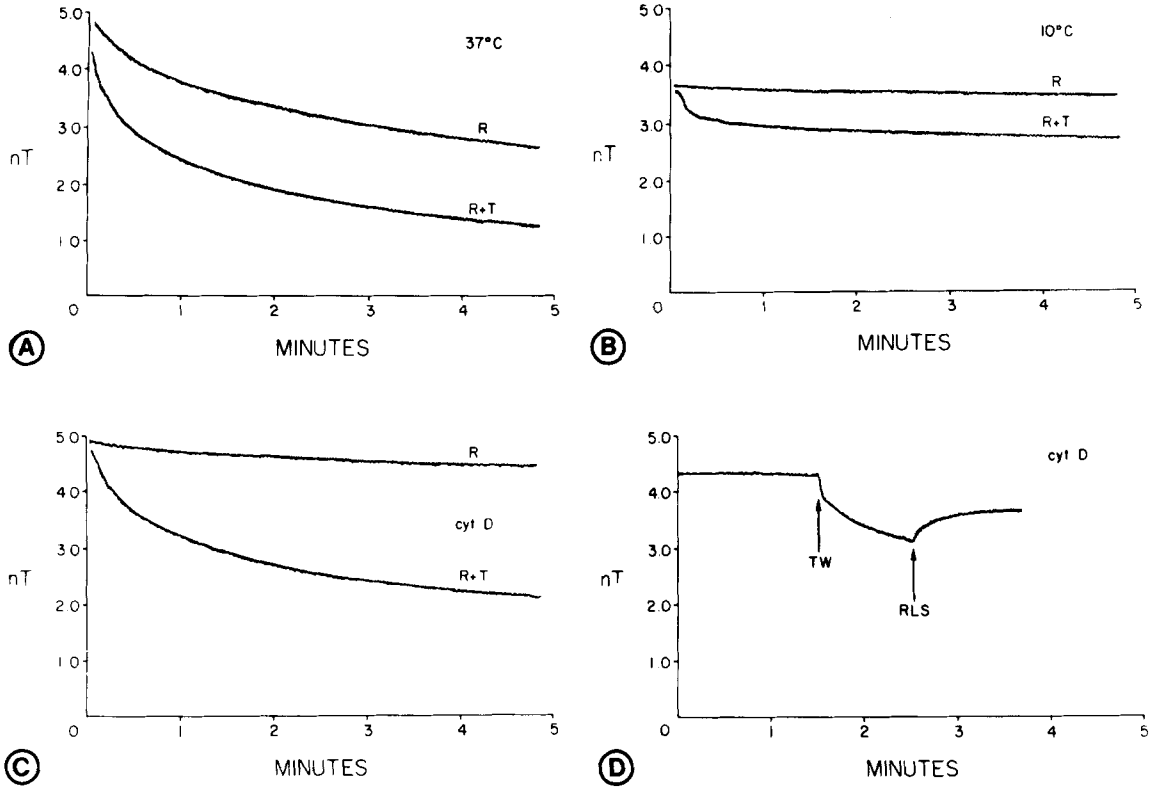

FIGURE 6 Graphs of the remanent magnetic field from maghemite-containing living cells after pulse (10 μs) magnetization. The upper curve (labeled *R*) in *A–C* shows the changes in remanent field that occur spontaneously in control cells at 37°C (*A*), cells cooled to 10°C (*B*), and cells treated with 20 μM cytochalasin D for 1 h (*C*). Inhibition of mechanisms moving particles is reflected by the reduced decay rate in *B* and *C* as compared to *A*. The lower curves (*R* + *T*) in *A–C* show the changes in remanent field when a 2.5-mT (25=G) twisting field is also applied at right angles to the initial direction of pulse magnetization with a strong field (100 mT =1,000 G). Cytoplasm at 10°C resists shear (*B*) whereas cytochalasin D-treated cytoplasm does not (C). Viscoelastic recoil of the cytoplasm could also be demonstrated (*D*). In *D*, the twisting field was applied at the time labeled *TW* (twist) and turned off at the time labeled *RLS* (release). The yield and recoil of the particle-containing organelles is evident.

sizes, and the larger ones contribute more to the remanent field in direct proportion to their larger mass (i.e., in proportion to the cube of their diameter). The effect on apparent viscosity measurement using rotation is minimal, however, since both the magnetic torque and viscous resistance to rotation increase as diameter cubed. Consequently, the effect of diameter on the observed magnetometric signal cancels out. Also, the effect of cell boundaries on particle rotation is small in that a 1-μm sphere rotating within a fixed 10-μm shell experiences a viscous drag only 0.1% larger than if it were in an infinite sea of material (9, 20). The effect of particle eccentricity up to a 5:1 ratio on the hydrodynamic diameter relevant to rotation is likewise small (<10%) (9).

It is important to remember that the maghemite particles are within phagosomes, so that the immediate environment of the particles is the vacuole interior (Fig. 3*C*). Since the exact site of shear is unknown, the measurements may be influenced by phagosomal contents. The magnetometrically measured apparent viscosity is an average over vesicles that may be variable in size, particle content, and protein content. The hydrodynamic diameter may be increased by the phagosome membrane and by attachment to other cell structures; these effects will make the measured viscosity larger than for freely rotating magnetic particles.

DISCUSSION

The study of cytoplasmic structure has commanded considerable attention in recent years owing to the widespread belief that the organized matrix of cytoskeletal fibers mediates many of the motile activities exhibited by cells. The historical and contemporary aspects of this endeavor have been thoroughly summarized recently (22, 26, 27). It is noteworthy, however, that few of these approaches directly address the physical properties of cytoplasm in relation to a particular motile activity. In this paper, we have presented results which suggest an alternative approach for probing cytoplasmic architecture which pertains to an organelle resident within the cytoplasm of macrophages. We have shown that alveolar macrophages readily engulf magnetic particles into phagosomal structures, and that subtle changes in the rotational mobility of particle-laden phagosomes can be magnetometrically detected. These signals can be used as an experimental indicator both of cytoplasmic activity and of the apparent cellular viscosity that retards motion of these organelles. Not only was it possible to estimate motion and viscosity for a discrete organelle with this technique, but it was found that the response of these organelles to an externally applied permanent magnet caused local alterations in the organization of the cytoskeleton that correlated well with other metabolic parameters of cell function. These findings are discussed with respect to other determinants of macrophage function and their potential application to a variety of problems in cell biology.

Macrophages have been widely studied because they are easy to obtain in large numbers and they exhibit pronounced

locomotory and phagocytic activities. Previous studies have shown that macrophages express a dynamically changing array of contractile proteins whose organization is regulated under a number of conditions including spreading, migration, and phagocytosis. For example, macrophage spreading on artificial substrates is accompanied by the deployment of actin into the cell cortex, particularly in regions of ruffles where membrane activity is exaggerated (1). Moreover, spreading can be enhanced by phorbol esters which amplify changes in the organization of other cytoskeletal fibers such as microtubules and intermediate filaments. Specifically, it has been noted that phorbol esters induce intermediate filament extension and the appearance of actin patches (24). By selectively perturbing the macrophage phagosomes with an external magnetic field, we have shown that f-actin and, to a lesser extent, intermediate filaments, are subjected to local changes in organization that presumably reflect the association of this organelle with these components of the cytoskeleton. Further support for this interpretation derives from observations that (*a*) the particle-loaded phagosomes are normally situated within intermediate filament cables as evidenced in transmission electron microscopy and immunofluorescence microscopy (see Figs. 3 and 5), (*b*) cytochalasin D, which caps the ends of actin filaments (21), impairs particle motions (see Fig. 6*C*), and (*c*) patches of actin appear upon particle alignment (see Fig. 5*D*). Although more work is needed to define the spatial relationships of phagosomes with the cytoskeleton, these studies suggest that both actin filaments and intermediate filaments may be partly responsible for the organelle movement detected. The observation that cytoplasmic microtubules are not affected by forced particle alignment implies that these structures are less involved in the regulation of phagosome organization.

Microtubules have been widely implicated in the guidance and motility of cytoplasmic organelles, but their participation may vary in different cell types (30). However, several observations relevant to the macrophage cytoskeleton pertain here. It is noteworthy that the fusion of lysosomes with phagosomes appears to occur predominantly in the perinuclear region (8), and our own video microscopy experiments indicate that most of the particle-laden phagosomes we have examined are perinuclear and apparently are unable to move translationally. Although microtubules appear to be essential in orienting macrophage lysosomes (24) and in centripetal movement (3), microtubules are not necessary for phagosome formation or fusion with lysosomes (3). The complexity in regulation owes in part to the many interactions that can exist between actin and microtubules (26) and microtubules and organelles (35). Although it has been proposed on the basis of in vitro experiments that MAP-2 can mediate binding of actin to microtubules (26), it is likely that such ATP-sensitive linkages are not involved in maintaining phagosomes within a perinuclear location. Rather, we envision these organelles to be embedded within a meshwork of f-actin and perhaps intermediate filaments which provides a barrier to translational movement and thus maintains them in a perinuclear position. Measurements of apparent local viscosity would then be a reflection of the maintenance of this structural matrix and would differ considerably from the matrix in the cortex where activity and structural rearrangements would involve primarily actin and its associated proteins (1, 44). Since cultured macrophages readily endocytose maghemite particles, it should be possible to probe cortical cytoplasm directly as a nascent phagosome is formed and is translocated to the perinuclear region.

These results are important in the interpretation of data obtained on the behavior of magnetic particles within intact organisms (4, 5, 7, 14, 15, 23). The phenomenon of remanent field decay after magnetization has been observed for magnetic particles retained in lungs of humans and animals, and has been termed "relaxation" (6). A number of speculations about the force driving relaxation have been put forward, including respiratory movements, surfactant and mucus flow, cardiac pulsations, particle diffusive motion, and cell motion. On the basis of a theoretical model of relaxation, Nemoto proposed that alveolar macrophage motility was the mechanism responsible for relaxation (23). Cytoplasmic activity was also implicated in the magnetometric study of Gehr et al. (14) in which magnetic particles were injected into the circulation and taken up by Kupffer cells in the liver. The correlation of videomicroscopy and magnetometry of isolated macrophages reported here provides more conclusive evidence that part of the remanent field decay observed for lungs in vivo can be attributed to intracellular motions within particle-containing pulmonary macrophages.

An earlier report on the relaxation phenomenon in isolated macrophages did not assess the contribution of Brownian movement to the motion detected (37). The application of a known external torque, as described here, can answer this question. From our estimates of apparent viscosity for control cells, we can calculate the contribution of Brownian movement to remanent field decay to be of the order of 9.2×10^{-4} min^{-1} (11). However, relaxation is observed to proceed at a much faster rate ($\sim 7.8 \times 10^{-2}$ min^{-1}) over the first fifteen minutes (see Fig. 6*A*). Thus, intracellular particles appear not to be driven primarily by thermal energy. Moreover, although various treatments have been found to influence cellular relaxation (37), an effect on active force generation in the cell could previously not be distinguished from an effect on intracellular apparent viscosity. From our viscosity results for 10°C and cytochalasin D–treated cells, it can be said that cooling the cells reduces motility by both disrupting force generation and increasing apparent viscosity (Fig. 6*B*), whereas cytochalasin D treatment only disrupts force generation and does not increase viscosity (Fig. 6*C*). The nature of the viscoelastic phenomenon (Fig. 6*D*) needs further characterization, but it reinforces the idea that the cell interior is not a simple Newtonian fluid but can both dissipate and store energy associated with particle displacements.

Previous investigations of cell viscosity (Table I) have used particles ranging from a very large size (~ 100 μm) (29) to molecular probes of small size (~ 0.003 μm) (22, 40, 42). The larger particles have been observed optically, and the molecules have been monitored by techniques that essentially measure their diffusion mobility. We used particles comparable in size to cell organelles (~ 0.3–0.7 μm) in conjunction with a non-optical method that is easier to quantitate for large numbers of cells. Furthermore, rather than examining reconstituted actin gels (44) or nonmammalian cells (17, 28, 29, 40, 43), our results apply to intact mammalian macrophages incubated at physiological conditions. It is clear from Table I that a wide range of apparent viscosities has been reported in a variety of cell systems. Some differences in results can be attributed to the non-Newtonian nature of the cytoplasm, i.e. as the shear rate goes down, the measured viscosity goes up. There also appears to be a trend that larger particles yield a larger relative viscosity. It must be kept in mind that all

TABLE I. *Experimental Measurements of Cytoplasmic Viscosity*

Investigators	Experimental Parameters				
	Cell system	Method	Particle diameter (μm)	Shear rate (s^{-1})	Apparent viscosity (poise)
Crick and Hughes, 1950[10]	Chick fibroblasts	Magnetic dragging, optical analysis	2-5	1.4	~10
Yagi, 1961[43]	Amoeba	Magnetic dragging, optical analysis	2-9	3.0	0.1-3
Hiramoto, 1969[17]	Sea urchin egg	Magnetic dragging, optical analysis	5-9	2-0.5	~100
King and Macklem, 1977[19]	(Airway mucus)	Oscillating particle, optical analysis	50-150	1.0	75
Wojcieszyn et al. 1981[42]	Foreskin fibroblasts	FPR	0.0072	2×10^4	0.8
Nemoto, 1982[23]	Particles in lungs	Response to magnetization	1.3	0.005	3,200-4,800
Sung et al. 1982[34]	Human neutrophils	Micropipette aspiration	(i.d. = 3)	0.01-0.02	~100
Wang et al. 1982[40]	Amoeba	FPR	0.0072	8×10^5	0.01-0.02
Sato et al. 1983[28]	Physarium	Magnetic dragging, optical analysis	4-16	0.5-3	1-5
Sato et al. 1984[29]	Squid axoplasm	Magnetic dragging, optical analysis	83-213	0.0001-0.004	10^5-10^6
Mastro and Keith, 1984[22]	Swiss 3T3 cell line	Electron spin resonance	0.00064	8×10^8	0.02
Valberg and Albertini*	Pulmonary macrophages	Magnetometry of twisted particles	0.3-0.7	0.001-0.003	$12\text{-}27 \times 10^3$

* This work.
Viscosity of H_2O = 0.007 poise at 37°C.
FPR, fluorescence photobleaching recovery.

measurements involving motion of a sphere in a non-Newtonian fluid are subject to difficulties in interpretation because even though the motion or rotation of the sphere in the fluid may be uniform, the shear rate is not, and changes with position on the surface of the sphere. In this type of situation, force (stress) and motion (strain) measurements cannot be unambiguously related to viscosity.

In our experiments, maghemite particles were twisted while contained in phagosomes. The possibility exists that particles can rotate within the phagosome, in which case the apparent viscosity is weighted by a contribution from the contents of the vacuole interior. If the phagosomal contents were of low viscosity, then our estimates of cytoplasmic apparent viscosity are too low, and should be considered only as a lower bound. However, we observed that cytochalasin D reduced apparent viscosity (Fig. 6*C*), and other studies have shown that the action of cytochalasin D is the disruption of cytoplasmic elements (21). This suggests that our method of examining viscosity is sensitive to structure in the cytoplasm. Moreover, the elastic recoil observed (Fig. 6*D*) is easier to understand as a property of cytoplasmic filaments rather than a property of proteases within the phagosomal interior. The effect of phagosome contents on the interpretation of viscosity measurements is less of a problem in particle translocation experiments (17, 28, 29, 43).

The spontaneous relaxation of remanent magnetization in maghemite-containing cells may prove useful as a non-invasive probe of cell viability. Whole animal studies have reported that the remanent field decay from magnetite in situ in lungs is changed when toxic particles are instilled into the lung (5). At the present time it is not known whether such changes are due to a direct effect of the toxic particles on macrophages, or whether toxic particles cause movement of the magnetite and/or macrophages to a different anatomical location where viscosity and freedom of movement are different. To understand this phenomenon, it will be necessary to undertake studies of how toxic effects in isolated cells are manifested in magnetometric signals.

In conclusion, magnetometry of isolated living cells can yield new information about both cytoplasmic motility and cytoplasmic physical properties, and can provide a means of probing organization of the cytoskeleton.

The anti-tubulin and anti-vimentin antibodies were kindly supplied by Drs. Keigi Fujiwara and Richard Hynes, respectively. We are grateful for the help and advice of Drs. Joseph Brain, Brian Herman, and Ann Watson as well as the technical assistance of Mr. Steve Bloom and Ms. Rebecca Stearns.

This work was supported by grants ES-00002, HL-29175, and HL-31029 to P. A. Valberg from the National Institutes of Health, and grant 82-17579 to D. F. Albertini from the National Science Foundation.

Received for publication 2 January 1985, and in revised form 25 March 1985.

REFERENCES

1. Amato, P. A., E. R. Unanue, and D. L. Taylor. 1983. Distribution of actin in spreading macrophages: a comparative study on living and fixed cells. *J. Cell Biol.* 96:750–761.
2. Barak, L. S., R. R. Yocum, E. A. Nothnagel, and W. W. Webb. 1980. Fluorescence staining of the actin cytoskeleton in living cells with 7-nitrobenz-2-oxa-1,3-diazole phallicidin. *Proc. Natl. Acad. Sci. USA.* 77:980–984.
3. Bhisey, A. N., and J. J. Freed. 1971. Altered movement of endosomes in colchicine-treated cultured macrophages. *Exp. Cell Res.* 64:430–438.
4. Brain, J. D., S. B. Bloom, P. A. Valberg, and P. Gehr. 1984. Correlation between the behavior of magnetic iron oxide particles in the lungs of rabbits and phagocytosis. *Exp. Lung Res.* 6:115–131.
5. Brain, J. D., T. Hu, and S. B. Bloom. 1984. Effects of SiO_2 and Fe_2O_3 on the clearance of magnetic particles from hamster lungs. *Am. Rev. Respir. Dis.* 129:A144.
6. Cohen, D. 1973. Ferromagnetic contaminants in the lungs and other organs of the body. *Science (Wash. DC).* 180:745–748.
7. Cohen, D., I. Nemoto, L. Kaufman, and S. Arai. 1984. Ferrimagnetic particles in the lung. Part II: The relaxation process. *IEEE (Inst. Electr. Electron. Eng.) Trans. Biomed. Eng.* 31:274–285.
8. Cohn, Z. A., M. E. Fedorno, and J. G. Hirsch. 1966. The *in vitro* differentiation of mononuclear phagocytes. V. The formation of macrophage lysosomes. *J. Exp. Med.* 127:757–766.
9. Crick, F. H. C. 1950. The physical properties of cytoplasm. A study by means of the magnetic particle method. Part II. Theoretical treatment. *Exp. Cell Res.* 1:505–533.
10. Crick, F. H. C., and A. F. W. Hughes. 1950. The physical properties of cytoplasm: a

study by means of the magnetic particle method. *Exp. Cell Res.* 1:37–80.
11. Einstein, A. 1926. Investigations on the theory of Brownian movement. Dover Publications. New York, NY. 31–34.
12. Fechheimer, M., and S. H. Zigmond. 1983. Changes in cytoskeletal proteins of polymorphonuclear leukocytes induced by chemotactic peptides. *Cell Motility.* 3:349–361.
13. Fujiwara, K., and T. D. Pollard. 1978. Simultaneous localization of myosin and tubulin in human tissue culture cells by double antibody staining. *J. Cell Biol.* 77:182–195.
14. Gehr, P., J. D. Brain, S. B. Bloom, and P. A. Valberg. 1983. Magnetic particles in the liver: a probe for intracellular movement. *Nature (Lond.).* 302:336–338.
15. Gehr, P., J. D. Brain, I. Nemoto, and S. B. Bloom. 1983. Behavior of magnetic particles in hamster lungs: estimates of clearance and cytoplasmic motility. *J. Appl. Physiol.: Respir. Environ. Exercise Physiol.* 55:1196–1202.
16. Herman, B., and D. F. Albertini. 1984. A time-lapse video image intensification analysis of cytoplasmic organelle movements during endosome translocation. *J. Cell Biol.* 98:565–576.
17. Hiramoto, Y. 1969. Mechanical properties of the protoplasm of the sea urchin egg. *Exp. Cell Res.* 56:201–208.
18. Hynes, R. O., and A. T. Destree. 1978. 10-nm filaments in normal and transformed cells. *Cell.* 13:151–163.
19. King, M., and P. T. Macklem. 1977. Rheological properties of microliter quantities of mucus. *J. Appl. Physiol.: Respir. Environ. Exercise Physiol.* 42:797–802.
20. Lamb, H. 1932. Hydrodynamics. Sixth edition. Dover Publications. New York, NY. 562–596.
21. MacLean-Fletcher, S., and T. D. Pollard. 1980. Mechanism of action of cytochalasin B on actin. *Cell.* 20:329–341.
22. Mastro, A. M., and A. D. Keith. 1984. Diffusion in the aqueous compartment. *J. Cell Biol.* 99:180s–187s.
23. Nemoto, I. 1982. A model of magnetization and relaxation of ferrimagnetic particles in the lung. *IEEE (Inst. Electr. Electron. Eng.) Trans. Biomed. Eng.* 29:745–752.
24. Phaire-Washington, L., S. C. Silverstein, and E. Wang. 1980. Phorbol myristate acetate stimulates microtubule and 10-nm filament extension and lysosome redistribution in mouse macrophages. *J. Cell Biol.* 86:641–655.
25. Pollard, T. D. 1981. Cytoplasmic contractile proteins. *J. Cell Biol.* 91:156s–165s.
26. Pollard, T. D., S. C. Selden, and P. Maupin. 1984. Interaction of actin filaments with microtubules. *J. Cell Biol.* 99:33s–37s.
27. Porter, K. R. 1984. The cytomatrix: a short history of its study. *J. Cell Biol.* 99:3s–12s.
28. Sato, M., T. Z. Wong, and R. D. Allen. 1983. Rheological properties of living cytoplasm: endoplasm of *Physarium* plasmodium. *J. Cell Biol.* 97:1089–1097.
29. Sato, M., T. Z. Wong, D. T. Brown, and R. D. Allen. 1984. Rheological properties of living cytoplasm: a preliminary investigation of squid axoplasm (*Loligo pealei*). *Cell Motility.* 4:7–23.
30. Schliwa, M. 1984. Mechanisms of intracellular organelle transport. *In* Cell and Muscle Motility. Volume 5. The Cytoskeleton. J. W. Shay, editor. Plenum Publishing Corp. New York. 1–82.
31. Sorokin, S. P. 1983. Dynamics of lysosomal elements in pulmonary alveolar macrophages. I. The postactivation lysosomal cycle. *Anat. Rec.* 206:117–143.
32. Sorokin, S. P. 1983. Dynamics of lysosomal elements in pulmonary alveolar macrophages. II. Transitory intracytoplasmic events in activated cells. *Anat. Rec.* 206:145–170.
33. Sorokin, S. P., and J. D. Brain. 1975. Pathways of clearance in mouse lungs exposed to iron oxide aerosols. *Anat. Rec.* 181:581–626.
34. Sung, K. P., W. Schmid-Schönbein, R. Skalak, B. Schuessler, U. Shunichi, and S. Chien. 1982. Influence of physicochemical factors on rheology of human neutrophils. *Biophys. J.* 39:101–106.
35. Supernant, K. A., and W. L. Dentler. 1982. Association between endocrine pancreatic secretory granules and in-vitro–assembled microtubules is dependent upon microtubule-associated proteins. *J. Cell Biol.* 93:164–174.
36. Taylor, D. L., and J. S. Condeelis. 1979. Cytoplasmic structure and contractility in amoeboid cells. *Int. Rev. Cytol.* 56:57–144.
37. Valberg, P. A. 1984. Magnetometry of ingested particles in pulmonary macrophages. *Science (Wash. DC).* 224:513–516.
38. Valberg, P. A., and J. D. Brain. 1979. Generation and use of three types of iron-oxide aerosol. *Am. Rev. Respir. Dis.* 120:1013–1024.
39. Valberg, P. A., B.-H. Chen, and J. D. Brain. 1982. Endocytosis of colloidal gold pulmonary macrophages. *Exp. Cell Res.* 141:1–14.
40. Wang, Y., F. Lanni, P. L. McNeil, B. R. Ware, and D. L. Taylor. 1982. Mobility of cytoplasmic and membrane-associated actin in living cells. *Proc. Natl. Acad. Sci. USA.* 79:4660–4664.
41. Weibel, E. R. 1980. *Stereological Methods, Vol. 2: Theoretical Foundations.* Academic Press, Inc. New York, NY. 175–214.
42. Wojcieszyn, J. W., R. A. Schlegel, E. S. Wu, and K. A. Jacobson. 1981. Diffusion of injected macromolecules within the cytoplasm of living cells. *Proc. Natl. Acad. Sci. USA.* 78:4407–4410.
43. Yagi, K. 1961. The mechanical and colloidal properties of Amoeba protoplasm and their relations to the mechanism of amoeboid movement. *Exp. Biochem. Physiol.* 3:73–91.
44. Zaner, K. S., and T. P. Stossel. 1982. Some perspectives on the viscosity of actin filaments. *J. Cell Biol.* 93:987–991.